



Validation of a Meteosat Second Generation solar radiation dataset over the northeastern Iberian Peninsula

J. Cristóbal¹ and M. C. Anderson²

¹Geophysical Institute, University of Alaska Fairbanks, 903 Koyukuk Dr. Fairbanks, Alaska, 99775-7320, USA

²Hydrology and Remote Sensing Laboratory, United States Department of Agriculture, Agriculture Research Service, BARC-West, Beltsville, Maryland, 20705, USA

Correspondence to: J. Cristóbal (jordi.cristobal@gi.alaska.edu)

Received: 9 July 2012 – Published in Hydrol. Earth Syst. Sci. Discuss.: 26 July 2012

Revised: 15 October 2012 – Accepted: 14 December 2012 – Published: 17 January 2013

Abstract. Solar radiation plays a key role in the Earth's energy balance and is used as an essential input data in radiation-based evapotranspiration (ET) models. Accurate gridded solar radiation data at high spatial and temporal resolution are needed to retrieve ET over large domains. In this work we present an evaluation at hourly, daily and monthly time steps and regional scale (Catalonia, NE Iberian Peninsula) of a satellite-based solar radiation product developed by the Land Surface Analysis Satellite Application Facility (LSA SAF) using data from the Meteosat Second Generation (MSG) Spinning Enhanced Visible and Infrared Imager (SEVIRI). Product performance and accuracy were evaluated for datasets segmented into two terrain classes (flat and hilly areas) and two atmospheric conditions (clear and cloudy sky), as well as for the full dataset as a whole. Evaluation against measurements made with ground-based pyranometers yielded good results in flat areas with an averaged model RMSE of 65 W m^{-2} (19%), 34 W m^{-2} (9.7%) and 21 W m^{-2} (5.6%), for hourly, daily and monthly-averaged solar radiation and including clear and cloudy sky conditions and snow or ice cover. Hilly areas yielded intermediate results with an averaged model RMSE (root mean square error) of 89 W m^{-2} (27%), 48 W m^{-2} (14.5%) and 32 W m^{-2} (9.3%), for hourly, daily and monthly time steps, suggesting the need of further improvements (e.g., terrain corrections) required for retrieving localized variability in solar radiation in these areas. According to the literature, the LSA SAF solar radiation product appears to have sufficient accuracy to serve as a useful and operative input to evaporative flux retrieval models.

1 Introduction

Knowledge of spatiotemporal distributions in solar radiation (R_s) is essential in many disciplines such as ecology, agronomy and hydrology, and plays a key role in the modeling of evapotranspiration (ET), both actual and potential, as well as air temperature. These variables are of high importance in monitoring and understanding the ecohydrological properties of terrestrial ecosystems and for agricultural support (Pons et al., 2012). Together with precipitation, ET is an essential variable in the hydrological cycle, and its modeling has been a research challenge over the last several decades (Dickinson, 1984; Manabe, 1969; Monteith, 1965). Currently, there is a wide variety of remote sensing models for calculating ET at regional or global scales that require R_s as an input (Allen et al., 1998, 2007; Anderson et al., 2004; Bastiaanssen et al., 1998; Cristóbal et al., 2011; Jackson et al., 1977; Kalma et al., 2008; Kustas and Norman, 2000; Priestley and Taylor, 1972; Roerink et al., 2000; Seguin and Itier, 1983). For operational applications, most of these methods try to minimize use of data from ground-based meteorological stations. Therefore, ET algorithms operating at regional to global scales can benefit from R_s surfaces retrieved using satellite imaging. Most of these ET methods have been validated in homogeneous covers (crops or natural vegetation) and flat areas, using a single value of R_s from a meteorological station record to describe a large area. However, in more complex terrain conditions, a single meteorological record may not be accurate enough to reasonably estimate ET spatially, considering gradients in the spatial distribution of R_s due to variable topography and cloud cover.

R_s is typically estimated using one of three different methodologies: empirical models, based on statistical correlations between R_s and other parameters; parametric models, based on the physics of interactions of R_s with the atmosphere (Martínez-Durbarán et al., 2009); and hybrid models that combine both approaches. Some of these models use GIS-based techniques and a digital elevation model, DEM, (Pons and Ninyerola, 2008) to compute R_s at regional and global scales in both simple and complex areas offering high accuracy and high spatial resolution, but relying on a well developed meteorological station network. In many regions, the density of meteorological stations is sparse and only satellites can realistically provide R_s data, especially at global scales (Journée and Bertrand, 2010; Olseth and Skartveit, 2001; Pinker et al., 2005).

Operational satellite systems provide valuable information on atmospheric parameters at regular intervals on a global scale. This satellite-based information greatly enhances our knowledge and understanding of the processes and dynamics within the Earth–atmosphere system. Nowadays, there is a wide variety of satellites, both geostationary and sun-synchronous, from which R_s can be retrieved regionally or globally such as Terra/Aqua Moderate Resolution Imaging Spectroradiometer (MODIS), the National Oceanic and Atmospheric Administration's (NOAA) Advanced Very High Resolution Radiometer (AVHRR), the Geostationary Operational Environmental Satellites (GOES) or the Meteosat Second Generation (MSG) Spinning Enhanced Visible and Infrared Imager sensor (SEVIRI). Unlike sun-synchronous sensors, geostationary sensors are especially interesting because of their high temporal resolution, which facilitates mapping of R_s at intervals of 15–30 min over large areas. In the case of Europe, there are currently three facilities that produce and offer R_s products from 30-min to monthly time steps derived from MSG SEVIRI data that can be used as input data in ET modeling: the Satellite Application Facility on Climate Monitoring, CM-SAF (<http://wui.cmsaf.eu/>), the Ocean and Sea Ice Satellite Application Facility, OSI SAF (<http://www.osi-saf.org/>), and the Land Surface Analysis Satellite Application Facility, LSA SAF (<http://landsaf.meteo.pt/>).

In this work we present a regional-scale evaluation of the LSA SAF R_s product, generated using MSG SEVIRI images from 2008 to 2011. The product dataset is evaluated at hourly, daily and monthly time steps, both as a whole and as subsets depending on terrain class (flat and hilly areas) and atmospheric conditions (clear and cloudy skies). In addition, the R_s product use as an input to evaporative flux retrievals is briefly discussed, as reported in the current literature.

2 Solar radiation product and model overview

Since 2007, the LSA SAF has offered an operative product describing the down-welling surface short-wave radiation

flux (DSSF), obtained by means of the SEVIRI sensor. The DSSF product preserves the projection and spatial resolution of the MSG SEVIRI images, using the ellipsoid normalized geostationary projection with a nominal spatial resolution of 3 km at nadir. This product is generated at a 30-min time step using data from the three solar spectrum channels of the SEVIRI sensor (centered on 0.6, 0.8 and 1.6 μm) and is encapsulated in an HDF5 file format. Each product file includes a set of three quality flag images (see Table 1): a land and sea mask, a cloud mask also including snow and ice cover; and the DSSF algorithm that was applied (clear or cloudy sky algorithm).

The model used to retrieve R_s for the DSSF product is based on the framework of the OSI SAF (Brisson et al., 1999) using three short-wave SEVIRI channels, 0.6 μm , 0.8 μm , and 1.6 μm (LSA SAF, 2010). The model is designed to compute the effective atmospheric transmittance, applying a clear or cloudy sky retrieval method depending on cloud cover. Cloud cover estimates are provided by the cloud mask developed by the nowcasting and very short-range forecasting, which is integrated in the LSA SAF operational system (Geiger et al., 2008b).

In the case of the clear sky method, the atmospheric transmittance and the spherical albedo of the atmosphere are calculated according to the methodology of Frouin et al. (1989). The water vapour used to estimate the atmospheric transmittance is obtained from the European Center for Medium-Range Weather Forecasts and the ozone amount is specified according to the Total Ozone Mapping Spectrometer climatology, while the visibility is currently kept at a fixed value of 20 km. The surface albedo is taken from the LSA SAF near-real-time albedo product (Geiger, 2008a).

In the case of the cloudy sky method, a simplified physical description of the radiation transfer in the cloud–atmosphere–surface system according to Gautier et al. (1980) and Brisson et al. (1999) is used. The cloud transmittance and albedo may be highly variable on small time scales depending on the daily evolution of the clouds. For this purpose the measured spectral reflectances in the 0.6 μm , 0.8 μm , and 1.6 μm SEVIRI are first transformed to broad-band top-of-atmosphere albedo by applying the spectral conversion relations proposed by Clerbaux et al. (2005) and the angular reflectance model of Manalo-Smith et al. (1998).

More information about the DSSF method can be found in Geiger et al. (2008b) and LSA SAF (2010).

3 Material and study area

3.1 Meteorological data

Hourly meteorological data were downloaded from the Catalan Meteorological Service (SMC) web (meteorological data are available at <http://ww.meteocat.com>). SMC currently manages a network of 165 meteorological ground stations in

Table 1. DSSF quality flag description.

Land/Sea mask	Cloud mask	DSSF algorithm
Ocean	Clear	Clear sky method
Land	Contaminated	Cloudy sky method
Space (outside of MSG disk)	Cloud filled	Night
Continental water	Snow/ice	Algorithm failed
	Undefined	Beyond specified view angle limit
	Unprocessed	Not processed (cloud mask undefined)

Table 2. Land cover type and altitude classes (in percentage) of the meteorological stations used in hourly, daily and monthly R_s evaluation.

Land use type	%	Altitude classes (m)	%
Natural vegetation	29	0–500	64
Crop areas	60	500–1000	23
Urban areas	11	1000–1500	4
		> 2000	9

Catalonia called the Meteorological Automatic Stations Network (XEMA). At its origin, XEMA combined several existing networks: the Agroclimatic Network, starting in 1996 and including 90 meteorological ground stations mainly covering crop field areas and with elevation ranging from 0 m to 1571 m; the Automatic Station Network, starting in 1988 and including 56 automatic meteorological ground stations covering natural vegetation and urban areas, ranging from 0 m to 1971 m; and starting in 1997, the Snow Meteorological Network which includes 8 automatic meteorological ground stations located over grasslands and covering high altitudes from 2200 m to 2540 m.

From the XEMA network, 140 meteorological stations measuring R_s were selected, applying a filter criterion consisting of stations that have been in service for at least 5 yr (see Fig. 1). For each of these stations SMC applies a data quality process and produces a R_s quality flag. The selected meteorological stations are located in different land uses and span a range in altitude (see Table 2), providing a broad basis for comparison with satellite retrievals under different circumstances.

In order to analyze the performance of the DSSF product in different terrain conditions, the meteorological stations were separated into two classes (see Fig. 1): those situated in flat and hilly terrain. This separation was based on a slope surface derived from a 30 m spatial resolution DEM from the *Institut Cartogràfic de Catalunya* (Cartographic Institute of Catalonia). The standard deviation in topographic slope was computed in a 3-km buffer area around each meteorological station, simulating the resolution of MSG SEVIRI. Slope standard deviation gives information about terrain heterogeneity, and whether or not the meteorological station is

surrounded by mountains that might influence shading of the R_s sensor. Based on these analyses, a threshold in slope standard deviation was selected to partition the network stations into two sets: 100 meteorological stations in relatively flat terrain, and 40 in hilly terrain.

3.2 DSSF product

A total of 1096 days of DSSF products for 2008 to 2010 were downloaded from the LSA SAF web site. A standard day consists of 48 files in HDF5 format, one image every 30 min, although there are days that have fewer files. In total, 52 608 files were downloaded and processed. To minimize impacts of data re-sampling due to reprojection, the analysis was carried out in the original projection and spatial resolution of the DSSF product.

4 Solar radiation extraction and evaluation criteria

Once the DSSF product was imported, data extraction was performed using bilinear interpolation in time between images and in space to meteorological station locations. Recent work in the literature suggests that averaging over a block of pixels centered on the location of a pyranometer significantly decreases the error compared to use of a single pixel, although there is no agreement on what is the optimal block size (Pinker and Laszlo, 1991; Rigollier et al., 2004; Journée and Bertrand, 2010). Nevertheless, in this work, we are interested in a pixel-based analysis to better capture effects of heterogeneity in the mountainous areas with narrow valleys found in our study area.

In order to manage data efficiently through the use of SQL statements, a database was built for product evaluation. This database consists of two parts: a DSSF record every 30 min, which incorporates both R_s and quality flags; and 1 h meteorological records that include measured R_s , data quality from the SMC and meteorological station terrain classes (flat or hilly).

DSSF evaluation was conducted using only pixels flagged as clear or cloudy (contaminated and cloud filled conditions) in the DSSF cloud mask and processed by clear and cloudy methods in the DSSF algorithm (see Table 1). Data under undefined and unprocessed categories in the DSSF cloud mask

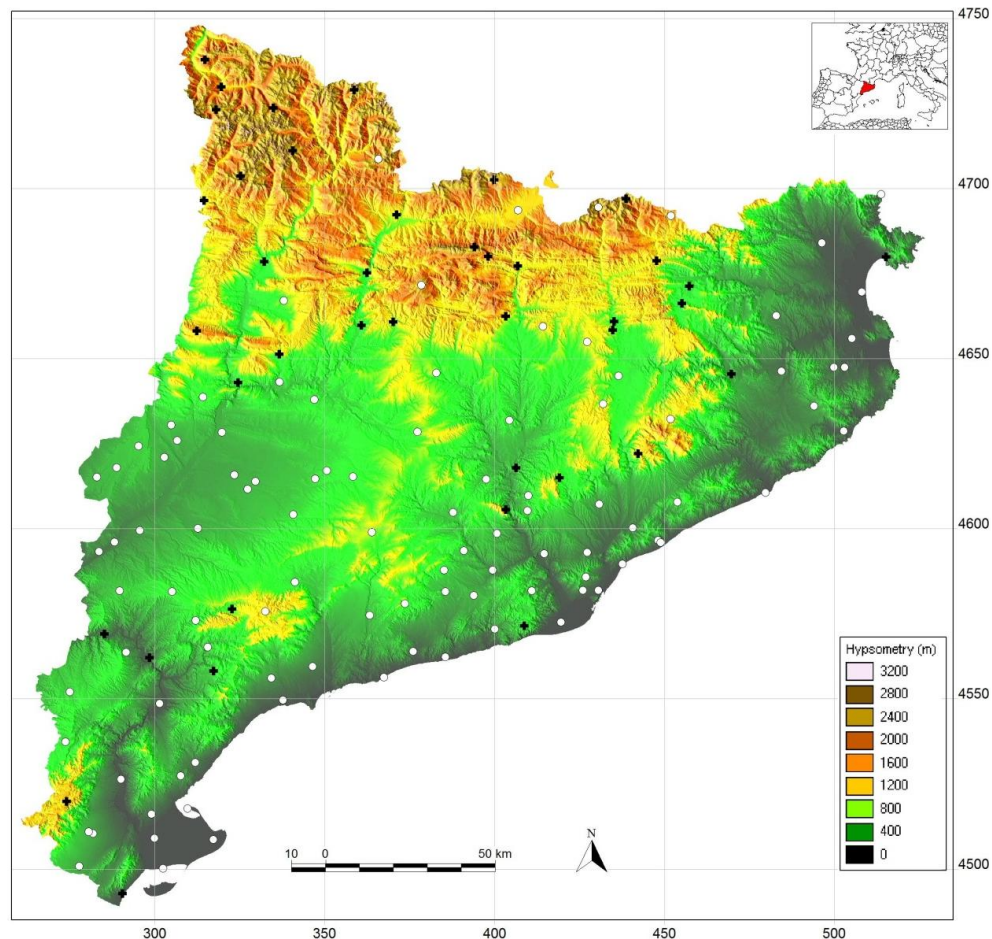


Fig. 1. Distribution of meteorological stations selected to validate the DSSF product depending on the terrain class: flat (white dots) and hilly (black crosses). Coordinates in UTM-31N and divided by 1000.

as well as algorithm failed, beyond specified view angle limit and not processed (cloud mask undefined) categories in the DSSF algorithm (see Table 1), representing less than 0.7 % for the whole dataset, were excluded from the analysis to avoid introducing errors in the evaluation analysis due to unreliable data.

In addition, images outside the interval between dawn and dusk (zero insolation) were also excluded from analysis in order not to magnify accuracy statistics. The calculation of dawn and dusk for each day and each meteorological station was carried out using the methodology proposed by Orús et al. (2007).

Based on these criteria, the DSSF product was evaluated with respect to ground observations at hourly, daily, and monthly timescales. This required aggregation of the DSSF product, available at 30 minute intervals, and the SMC R_s data, available only at hourly intervals. For hourly evaluation, DSSF algorithm performance was analyzed under both clear and cloudy sky conditions and snow and ice cover. To focus on pixels where cloud conditions were relatively sta-

ble over the hourly sampling interval of the SMC dataset, the hourly evaluation was conducted using only pixels reporting the same quality flags during each hourly interval in terms of cloud mask and DSSF algorithm (i.e., a pixel masked as clear both at 12:00 UTC and 12:30 UTC). On the other hand, pixels with different quality flags for a specific hour were excluded in the analysis (i.e., a pixel masked as clear at 12:00 UTC and cloudy at 12:30 UTC).

The relative performance of the clear and cloudy sky algorithms used in the DSSF process was also explored. Currently, there is no agreement on how to best define a clear-sky day in terms of amount of cloud-free time. In this study, a clear-sky day at a given pixel was defined such that $\geq 80\%$ of the time samples between dawn and dusk were cloud free. Moreover, as criteria for computation of daily average R_s from the DSSF product, we specified that at least 90 % of the potential images within a day must be available. A similar criterion of completeness was applied to the pyranometer data, but requiring all data samples from dawn to dusk to have a good quality flag. Finally, in the case of

Table 3. Hourly solar radiation error and accuracy statistics depending on flat or hilly terrain, clear and cloudy sky conditions, and presence of snow or ice cover from 2008 to 2010. RMSE, MBE and MAE in $W m^{-2}$, PE in percentage and n is the number of samples.

Flat terrain							Hilly terrain						
All sky	RMSE	R^2	PE	MBE	MAE	n	All sky	RMSE	R^2	PE	MBE	MAE	n
2008	71	0.94	22	-2	44	379 862	2008	90	0.90	29	-1	55	129 058
2009	62	0.96	18	-6	40	386 098	2009	88	0.91	26	-9	56	144 949
2010	61	0.96	18	-7	39	386 547	2010	88	0.91	27	-6	56	147 568
2008–2010	65	0.95	19	-5	41	1 152 507	2008–2010	89	0.91	27	-6	56	421 575
Clear sky	RMSE	R^2	PE	MBE	MAE	n	Clear sky	RMSE	R^2	PE	MBE	MAE	n
2008	43	0.98	10	-4	30	201 260	2008	60	0.96	15	-5	38	60 040
2009	41	0.98	9	-3	28	218 139	2009	63	0.96	15	-3	38	69 226
2010	40	0.98	9	-7	27	212 747	2010	63	0.96	16	-6	38	65 515
2008–2010	41	0.98	10	-5	28	632 146	2008–2010	62	0.96	15	-4	38	194 781
Cloudy sky	RMSE	R^2	PE	MBE	MAE	n	Cloudy sky	RMSE	R^2	PE	MBE	MAE	n
2008	93	0.85	40	0	59	178 371	2008	109	0.80	46	1	70	67 771
2009	82	0.88	35	-9	55	167 245	2009	106	0.82	41	-14	71	72 140
2010	80	0.89	33	-7	54	172 238	2010	102	0.84	40	-6	69	78 505
2008–2010	85	0.87	36	-5	56	517 854	2008–2010	106	0.82	42	-7	70	218 416
Snow/Ice	RMSE	R^2	PE	MBE	MAE	n	Snow/Ice	RMSE	R^2	PE	MBE	MAE	n
2008	104	0.77	33	-16	85	231	2008	133	0.64	46	23	104	1247
2009	107	0.79	28	-20	90	714	2009	115	0.84	25	-27	93	3583
2010	92	0.85	20	-17	69	1562	2010	119	0.83	26	-8	91	3548
2008–2010	98	0.84	23	-18	77	2507	2008–2010	119	0.82	27	-11	94	8378

monthly aggregation, no distinction was made between clear or cloudy conditions given the length of the averaging interval. A criterion of having daily aggregates in both satellite product and pyranometer datasets for more than 25 days per month was enforced to ensure that these data were representative of monthly conditions.

5 Accuracy and error estimation

The performance of the DSSF product was evaluated using several statistical indices and measures of error. The coefficient of determination (R^2) indicates the precision of the estimates in relation to measured R_s , the root mean square error (RMSE, Eq. 1) is used to measure the differences between values predicted by a model or an estimator and the values actually observed and is a measure of accuracy, the mean absolute error (MAE, Eq. 2) indicates the magnitude of the average error, the mean bias error (MBE, Eq. 3) indicates cumulative offsets between measured and observed values, and the percentage of error (PE, Eq. 4) expresses the magnitude of the error between observed and estimated values relative to the observed mean value:

$$RMSE = \sqrt{\frac{\sum_{i=1}^n (e_i - o_i)^2}{n}}, \tag{1}$$

$$MAE = \frac{\sum_{i=1}^n |e_i - o_i|}{n}, \tag{2}$$

$$MBE = \frac{\sum_{i=1}^n (e_i - o_i)}{n}, \tag{3}$$

$$PE = 100 \left(\frac{1}{\bar{X}} \sqrt{\frac{\sum_{i=1}^n (e_i - o_i)^2}{n}} \right), \tag{4}$$

where e_i refers to the estimated value of the variable in question (satellite-derived R_s), o_i is the observed value (in situ R_s measurement provided by the meteorological station), n is the number of datapoints, and \bar{X} is the average of the n o_i values.

Table 4. Daily solar radiation error and accuracy statistics depending on flat or hilly terrain and clear sky or cloudy sky conditions from 2008 to 2010. RMSE, MBE and MAE in W m^{-2} , PE in percentage and n is the number of samples.

Flat terrain							Hilly terrain						
All sky	RMSE	R^2	PE	MBE	MAE	n	All sky	RMSE	R^2	PE	MBE	MAE	n
2008	27	0.95	11.6	-9	22	30 241	2008	39	0.92	15.6	-9	28	10 295
2009	25	0.97	8.8	-7	20	29 865	2009	39	0.93	14.0	-6	28	11 223
2010	35	0.97	8.6	-5	25	30 472	2010	50	0.93	14.0	-5	36	11 512
2008–2010	34	0.96	9.7	-6	24	90 578	2008–2010	48	0.93	14.5	-5	35	33 030
Clear sky	RMSE	R^2	PE	MBE	MAE	n	Clear sky	RMSE	R^2	PE	MBE	MAE	n
2008	27	0.98	6.1	-9	22	8253	2008	38.6	0.96	8.6	-9	28	2324
2009	25	0.97	5.5	-7	20	8384	2009	38.8	0.94	8.3	-6	28	2440
2010	25	0.98	5.6	-11	20	8869	2010	42.5	0.95	9.0	-9	29	2431
2008–2010	26	0.98	5.7	-9	21	25 506	2008–2010	40.0	0.95	8.6	-8	28	7195
Cloudy sky	RMSE	R^2	PE	MBE	MAE	n	Cloudy sky	RMSE	R^2	PE	MBE	MAE	n
2008	43	0.93	14.1	0	28	21 988	2008	53	0.90	18.3	0	37	7971
2009	33	0.96	10.7	-6	25	21 481	2009	50	0.92	16.2	-9	36	8783
2010	32	0.97	10.3	-6	24	21 603	2010	48	0.92	16.0	-5	36	9081
2008–2010	36	0.95	11.9	-4	26	65 072	2008–2010	50	0.91	16.8	-5	36	25 835

6 Evaluation results and discussion

6.1 Hourly evaluation

Table 3 shows results of statistical evaluation at hourly time steps, with data segmented based on terrain classes (flat or hilly), clear or cloudy sky conditions, as well as presence of snow and ice cover, by year and averaged from 2008 to 2010. The RMSE variability for all sky conditions from 2008 to 2010 is low in both terrain classes, not exceeding more than 10 W m^{-2} (from 61 W m^{-2} to 71 W m^{-2}) in flat sites and 2 W m^{-2} (from 88 W m^{-2} to 90 W m^{-2}) in hilly sites (number of samples is similar in both cases). High R^2 values (> 0.8) also indicate a strong agreement between DSSF and meteorological station data. However, apparent satellite retrieval performance shows a significant dependence on local terrain conditions, with better agreement with observations in flat areas for all analyzed years. In terms of RMSE, the difference in accuracy between hilly and flat classes is about 24 W m^{-2} . This behavior is expected, and might be due either to actual errors in the retrieval or errors in representativeness of the point pyranometer observations with respect to R_s levels averaged over the surrounding 3 km pixel. To fully understand remote sensing R_s behavior in hilly terrain areas, further research needs to be addressed in order to evaluate the representativeness of the point pyranometer observations with remote sensing R_s measurements. When datasets are segmented based on both atmospheric conditions and terrain classes, clear sky conditions show better measurement agreement than cloudy conditions (2008–2010) in both flat and hilly sites. Averaged over the period 2008–2010, for flat terrain differences between cloudy and clear sky conditions

in terms of RMSE, MAE and PE are 44 W m^{-2} , 28 W m^{-2} and 26 %, respectively. In the case of hilly terrain these differences are 44 W m^{-2} , 32 W m^{-2} and 37 %, respectively. Finally, for snow and ice covers these differences between hilly and flat classes in terms of RMSE, MAE and PE are 21 W m^{-2} , 17 W m^{-2} and 4 %, respectively. It is interesting to note that in most of the cases MBE is negative, meaning that the DSSF algorithm underestimates R_s measured at the pyranometer, although mean MBE values for the averaged 2008–2010 period and for all conditions do not exceed -6 W m^{-2} .

A literature review reveals only three comparative studies that clearly address the issue of terrain conditions on R_s product evaluation. The use of different accuracy and error estimators, as well as differences in temporal extent of analysis and thresholding criteria, complicates a detailed comparison of the results presented here with those in other references. Nevertheless, a qualitative comparison with prior results provides some useful context for the current study.

In the case of flat conditions (column 1 in Table 3), the evaluation results presented here are in agreement with those found in the literature. In the DSSF product validation performed by Geiger et al. (2008b), with data of 6 meteorological stations from 2004 to 2006, a RMSE of 40 W m^{-2} and 110 W m^{-2} was found for clear sky and cloudy sky conditions, respectively; and a MBE of 9 W m^{-2} and 5 W m^{-2} , respectively. Journée and Bertrand (2010) reported an overall RMSE for clear sky and cloudy sky conditions of 110 W m^{-2} using 13 meteorological stations in Belgium from 2008 to 2009 when using DSSF data. In comparison, focusing on stations in flat terrain, RMSE of 41 W m^{-2} and 85 W m^{-2} are

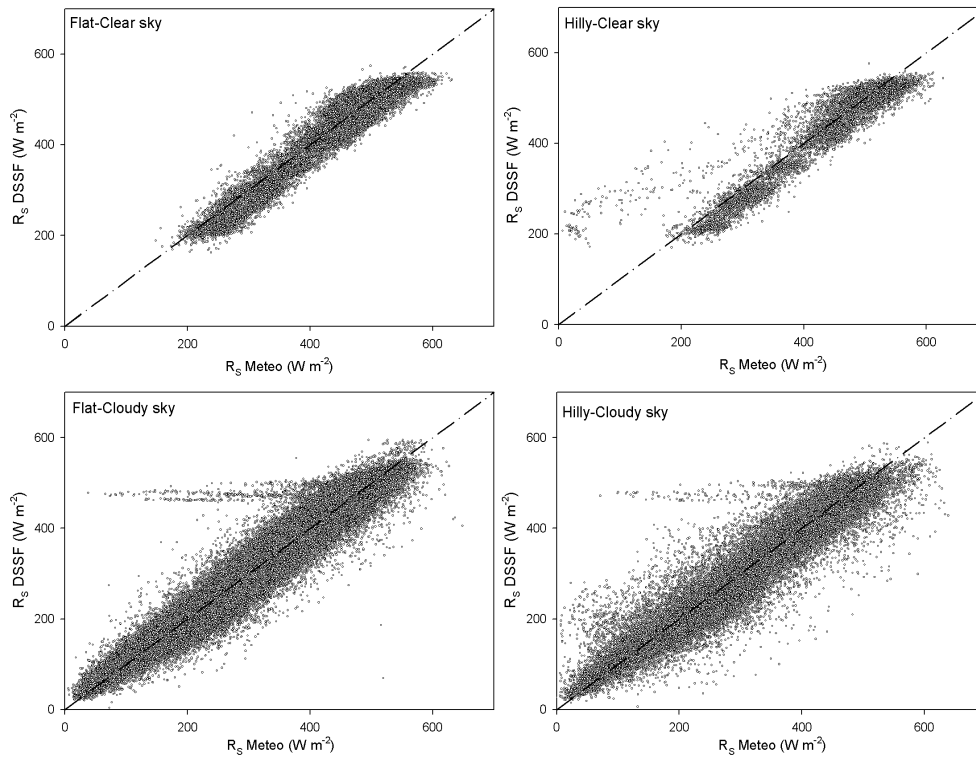


Fig. 2. Daily DSSF solar radiation (R_s DSSF) vs. daily solar radiation measured at meteorological stations (R_s Meteo) for 2008 to 2010, segmented into subsets based on flat/hilly terrain and clear/cloudy sky condition. Solid line is the 1 : 1 ratio.

found for clear and cloudy conditions, with MBE of 5 W m^{-2} in both cases. Improvement in RMSE in the current study may be due to further product improvement in 2010, or to differences in data rejection criteria.

Comparing all satellite application facility irradiance products (CM-SAF, OSI SAF and LSA SAF) at 15 km of spatial resolution, including also the DSSF product, Ineichen et al. (2009) found a RMSE between 80 W m^{-2} and 100 W m^{-2} and a PE ranging from 15 % to 32 % using 8 meteorological stations over Europe. According to Rigollier et al. (2004), the obtained hourly results are within the error displayed by Heliosat-1 and Heliosat-2 models, also designed for Meteosat images, and reported RMSE errors from 64 W m^{-2} to 120 W m^{-2} and a PE from 7 % to 16 % in the case of Heliosat-1 hourly irradiation. In the same work, they reported an hourly irradiation RMSE and PE from 62 W m^{-2} to 103 W m^{-2} and from 18 % to 45 %, respectively, using the Heliosat-2 algorithm in three months from 1994 to 1995 and using 35 stations in flat areas, ranging the bias from -31 W m^{-2} to 1 W m^{-2} . Using GOES-W and GOES-E data, Otkin et al. (2005) report a PE, a RMSE and a MBE of 19 %, 62 W m^{-2} and -2 W m^{-2} , respectively, using observations from 11 meteorological stations from the US Climate Reference Network over a continuous 15-month period at 20 km of spatial resolution; and Garautza-Payan et al. (2001) reported similar results in northern Mexico of about 13 % of PE and

69 W m^{-2} of RMSE in a one year experiment using data from 2 flux towers.

In general terms, the presence of snow or ice yielded in higher MBE, RMSE and lower correlation, especially in hilly sites. Dürr et al. (2010) also found a large negative MBE on the order of 15 W m^{-2} to 25 W m^{-2} over the alpine region using the CM-SAF solar radiation product. In this case, the snow and ice surface albedo may be difficult to define, leading to higher errors compared to other land covers and according to Dürr et al. (2010) a dynamic snow-albedo map could improve the solar radiation retrieval in snow covered areas. Still, R^2 values of ~ 0.8 indicate that useful data are being generated even for these difficult land cover situations.

It is worth remarking that the mean PE obtained in this study at hourly time steps for all atmospheric conditions in flat and hilly classes was 19 % and 27 %, respectively, and according to Zelenka et al. (1999) this value compares favorably with the value from 20 % to 25 % reported world-wide. While PE during cloudy sky conditions exceeds this range, with values of 36 % and 42 % respectively, this is mostly a function of lower mean observed R_s during periods of cloud cover. Finally, DSSF values over snow and ice cover also yield a PE in this interval, ranging from 23 % to 27 %.

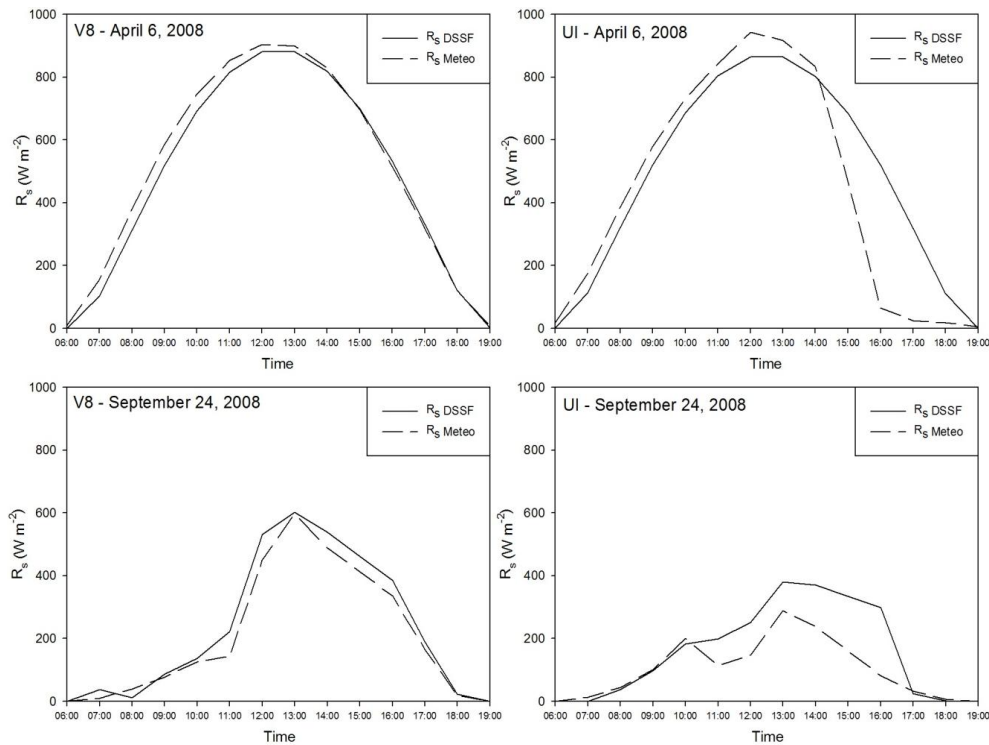


Fig. 3. Examples of daily solar radiation cycle from dawn to dusk at two meteorological stations located in flat conditions (V8) and hilly conditions (UI) during a clear sky day (6 April 2008) and cloudy sky day (24 September 2008). Time in UTC.

6.2 Daily evaluation

Table 4 shows evaluation results of daily time steps, depending on terrain class and sky conditions, averaged by year and from 2008 to 2010. Scatter plot comparisons for 2008–2010 are shown in Fig. 2. Results at the daily interval show similar general behavior with the hourly results. DSSF data retrieved over flat sites in both clear and cloudy sky conditions show better agreement with observations than retrievals over hilly sites. At flat sites, clear sky conditions yield an averaged RMSE, MAE, PE and R^2 for the 2008–2010 period of 26 W m^{-2} and 21 W m^{-2} , 5.7 % and 0.98, respectively; and cloudy sky conditions an averaged RMSE, MAE, PE and R^2 for the 2008–2010 period of 36 W m^{-2} and 26 W m^{-2} , 11.9 % and 0.95, respectively. For hilly sites, clear sky conditions yield an averaged RMSE, MAE, PE and R^2 for the 2008–2010 period of 40 W m^{-2} and 28 W m^{-2} , 8.6 % and 0.95, respectively; and cloudy sky conditions an averaged RMSE, MAE, PE and R^2 for the 2008–2010 period of 50 W m^{-2} and 36 W m^{-2} , 16.8 % and 0.91, respectively.

Figure 3 shows examples of daily R_s dynamics from dawn to dusk at two meteorological stations located in flat (V8) and hilly terrain (UI) during a clear sky day (both on 6 April 2008) and a cloudy sky day (24 September 2008). The upper left plot shows the best-case scenario, for the site in flat terrain under clear sky, while the upper right shows data for the same clear day at the site in hilly terrain. The

hilly site shows evidence of topographic shadows between 16:00 UTC and 19:00 UTC, while the 3-km average does not show a strong diurnal shadowing effect. According to a sensitivity analysis by Oliphant et al. (2003), to isolate the role of spatial variability of surface characteristics in generating variance in the radiation budget, one of most important characteristics was found to be slope aspect. This fact suggests that in hilly sites, the DSSF algorithm could be enhanced to reproduce sub-pixel variability in shadowing effects by accounting for topography using a DEM.

The lower plots in Fig. 3 show daily R_s dynamics under cloudy sky conditions for both flat and hilly sites. As seen in Table 4, the accuracy of the DSSF algorithm is lower under cloud cover relative to the clear-sky case. Still, in this case the DSSF algorithm reproduces the meteorological station R_s dynamics with reasonable fidelity at the flat site.

As in the hourly evaluation case, the MBE is negative in almost all cases, meaning that on average the DSSF algorithm underestimates R_s at the daily timescale, although the bias determined for both terrain classes for the averaged 2008–2010 period does not exceed -6 W m^{-2} .

Results presented here at the daily time step are consistent with those found in the literature. Bois et al. (2008) reported a RMSE of 2.16 MJ m^{-2} and a PE of 14 % using a Meteosat R_s product obtained by means of the Heliosat-2 method in comparison with daily data from 19 meteorological stations in flat areas from 2000 to 2004. With the same method applied

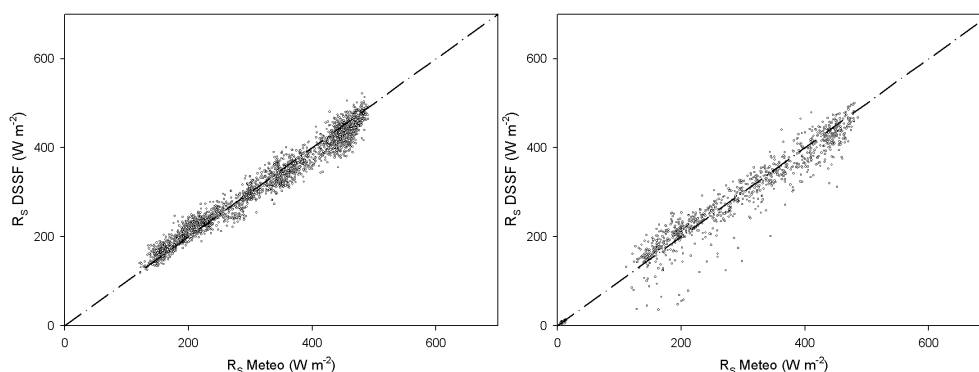


Fig. 4. Monthly DSSF solar radiation (R_s DSSF) vs. monthly meteorological station solar radiation (R_s DSSF) from 2008 to 2010, segmented into flat or hilly terrain classes. Solid line is the 1 : 1 ratio.

to Meteosat data, Rigollier et al. (2004) found a PE between 9 % and 20 % in his dataset as well as for other works using the same method. Using GOES, Otkin et al. (2005) found a RMSE of 15.5 W m^{-2} and a MBE of -1.1 W m^{-2} over the US, Garautza-Payan et al. (2001) a PE of 11.7 %, and Paech et al. (2009) a PE of 10 %.

6.3 Monthly evaluation

Table 5 and Fig. 4 show results from comparison of satellite retrievals and pyranometer data aggregated to monthly time steps. Comparisons at sites in flat terrain yield an averaged RMSE, MAE, PE and R^2 for the 2008–2010 period of 21 W m^{-2} and 17 W m^{-2} , 5.6 % and 0.99, respectively; while hilly sites yield an averaged RMSE, MAE, PE and R^2 of 32 W m^{-2} and 23 W m^{-2} , 9.3 % and 0.97, respectively. As with the hourly and daily results, better agreement was obtained at sites in flat terrain, although dependency of accuracy on terrain condition was not as marked at the monthly time step. In both cases, MBE is negative in all cases meaning that on average the DSSF algorithm underestimates R_s at the monthly timescale, although the bias determined for both terrain classes for the averaged 2008–2010 period does not exceed -5 W m^{-2} . Using the DSSF product, Geiger et al. (2008a) found no clear seasonal bias dependence in the results. However, seasonal trends in MBE show that MBE is generally more positive during summer months, from June to September, and negative for the rest of the year in flat and hilly sites (see Fig. 5). Pinker et al. (2003) and Otkin et al. (2005) also found similar seasonal trends in MBE using GOES to model R_s . According to Geiger et al. (2008a) and Ineichen et al. (2009) this bias may be related to the atmospheric transmission inputs such as the atmospheric turbidity that could be addressed by considering the temporal and spatial variability of the aerosol concentration in more detail. The removal of this bias would further decrease the RMSE and the MBE in model estimates for both terrain classes.

Figure 6 shows an example of the monthly DSSF solar radiation (R_s DSSF) and monthly meteorological station solar radiation (R_s DSSF) cycle from 2008 to 2010 at two meteorological stations located in flat conditions (DP) and hilly conditions (WQ). In general, the DSSF product reasonably reproduces the seasonal variability measured at these two meteorological stations, located in both a flat and hilly landscape.

These monthly results are in good agreement with previous work, although there are few studies that have aggregated R_s on a monthly basis. Rigollier et al. (2004) reported a PE from 5 % to 24 % based on their dataset as well as for other studies using the same retrieval method. Using Meteosat retrievals, Pereira et al. (1996) reported a PE of 13 % during a 2-yr period (1985–1986) and using 22 meteorological stations. Finally, using data from GOES, GMS and MT-SAT from 1995 to 2008, Janjai et al. (2011) found a PE of 6.3 % with 5 meteorological stations in flat areas in Cambodia. According to Pinker et al. (2005), several attempts to compute R_s with remote sensing data at a monthly time step and at a global scale yielded RMSE between 11.7 W m^{-2} and 31.5 W m^{-2} .

It is interesting to remark that similar results were found by Pons and Ninyerola (2008) using a hybrid model, applying DEM-based corrections to R_s retrievals and comparing to 5 yr series of monthly data from meteorological stations. They found a PE ranging from 7.3 % to 13.1 % in four months, with a RMSE from 20 W m^{-2} to 24 W m^{-2} . If we take also into account that 77 % of the meteorological stations analyzed present a complete 3-yr monthly R_s record from the DSSF, then this means that this product can be also useful for mapping R_s from a climatic perspective (Cristóbal et al., 2008; Ninyerola et al., 2000).

6.4 Using DSSF as input data in ET modeling

While few analyses of ET model sensitivity to R_s accuracy have been published, Diak et al. (2004) claim that a PE about 10 % or less for daily solar radiation is acceptable

Table 5. Monthly solar radiation error and accuracy statistics for 2008 to 2010 by terrain class. RMSE, MBE and MAE in W m^{-2} , PE in percentage and n is the number of samples.

	Flat terrain						Hilly terrain						
	RMSE	R^2	PE	MBE	MAE	n	RMSE	R^2	PE	MBE	MAE	n	
2008	25	0.99	6.0	-6	0.8	877	2008	33	0.96	9.2	-6	24	313
2009	18	0.99	5.6	-1	0.7	779	2009	31	0.97	9.6	0	22	282
2010	21	0.99	5.2	-6	0.7	915	2010	32	0.96	9.2	-6	23	341
2008–2010	21	0.99	5.6	-4	0.7	2571	2008–2010	32	0.97	9.3	-5	23	936

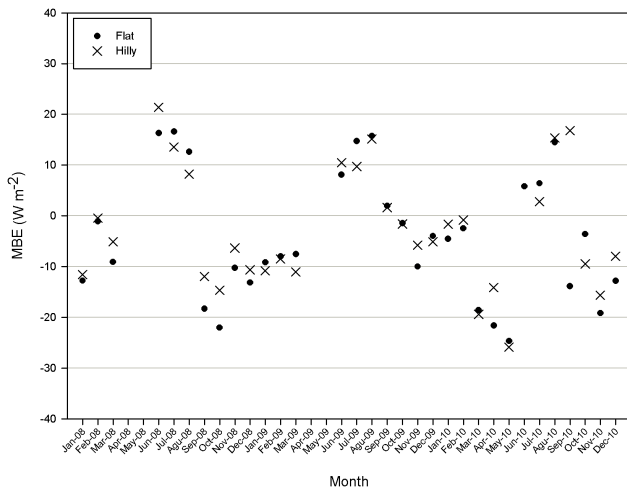


Fig. 5. Monthly MBE from 2008 to 2010 in flat and hilly terrain classes.

for reasonable model performance. When retrieving net radiation, an essential variable for estimating ET, Kustas et al. (1994), found that daily GOES R_s data with a RMSE of 23 W m^{-2} led to acceptable basin-scale estimates. In the work of Diak et al. (1998), R_s derived from GOES was applied to routinely estimate daily crop ET for irrigation scheduling in Wisconsin, USA. Stewart et al. (1999) used GOES data to retrieve hourly and daily R_s in a comparison among three evapotranspiration formulations applied over an agricultural area in northwest of Mexico. They found that hourly PE of 9.1 % and 16.8 % for clear sky and all averaged conditions, respectively, and daily PE of 4.7 % and 9.2 % for clear sky and all averaged conditions, respectively, produced reasonable estimates of ET. Garautza-Payan et al. (2001) and Garautza-Payan and Watts (2005) estimated crop water requirements of irrigated vegetation, cotton and wheat, in the same area also using GOES data as the R_s input for ET modeling. The GOES derived R_s data displayed a PE from 9 % to 14 % and from 7 % to 14 % for hourly and daily periods, respectively, allowing retrieval of daily cotton and wheat ET with a RMSE of 23 W m^{-2} and 7 W m^{-2} , respectively. In the work conducted by Jacobs et al. (2002), GOES data was used to estimate wetland potential ET in Florida, USA,

during a growing season under non-water-limited conditions. R_s evaluation with ground data showed a PE of 28.3 % and 9.9 % for 30-min and daily R_s time steps, yielding an ET error at 30-min time steps of around 30 % and a R^2 of 0.67 but lower error of 3.1 % and higher R^2 of 0.90 in daily ET retrievals. When comparing four potential ET methods at a daily time step over a wetland area in Florida, USA, Jacobs et al. (2004) found dramatic improvements in the efficiency of ET-radiation based models using GOES R_s , with a RMSE of 19.4 W m^{-2} . During the soil-moisture atmospheric coupling experiment (SMACEX) carried out in Iowa, USA, in 2002, Su et al. (2005) reported good agreement between modeled ET using GOES R_s data and in situ observations of instantaneous ET, with a RMSE of 60 W m^{-2} in 8 corn and soybean plots. In evaluating crop reference ET estimation at a daily time step in two study areas in southern France, Bois et al. (2008), found better results from methods using Meteosat R_s compared to methods only using air temperature, ranging the relative annual RMSE from 22 % to 28 %, according to the method and the type of climate, humid-Oceanic or semi-arid Mediterranean. Using a calibrated R_s product derived from GOES data with a PE of 10 % (1.7 MJ m^{-2}) for daily reference and potential ET in Florida, USA, Paech et al. (2009) estimated an error from 5 % to 6 % in potential ET retrieval, generating a product useful for routine water management-related activities.

In general terms, evaluation results derived from this study show that the DSSF product has a relative error of about 10 % in comparison with pyranometer data at daily time steps, and according to the literature, can be used as a functional input to radiation-based ET models. However, in order to fully understand the sensitivity of modeled ET to satellite-derived R_s uncertainty, an error analysis should be conducted for each ET model.

It is important to remark that DSSF products may produce errors in models running at finer spatial scales (sub 3-km) over regions of hilly terrain unless topographic corrections are applied. This may be important for ET modeling applied to Landsat thermal imagery from 60 m to 100 m spatial resolution. Errors are significantly higher over regions of snow cover, and this could affect studies monitoring energy fluxes and snow melt in cold land regions. At daily time steps, the DSSF product performs within the 10 % error, except for

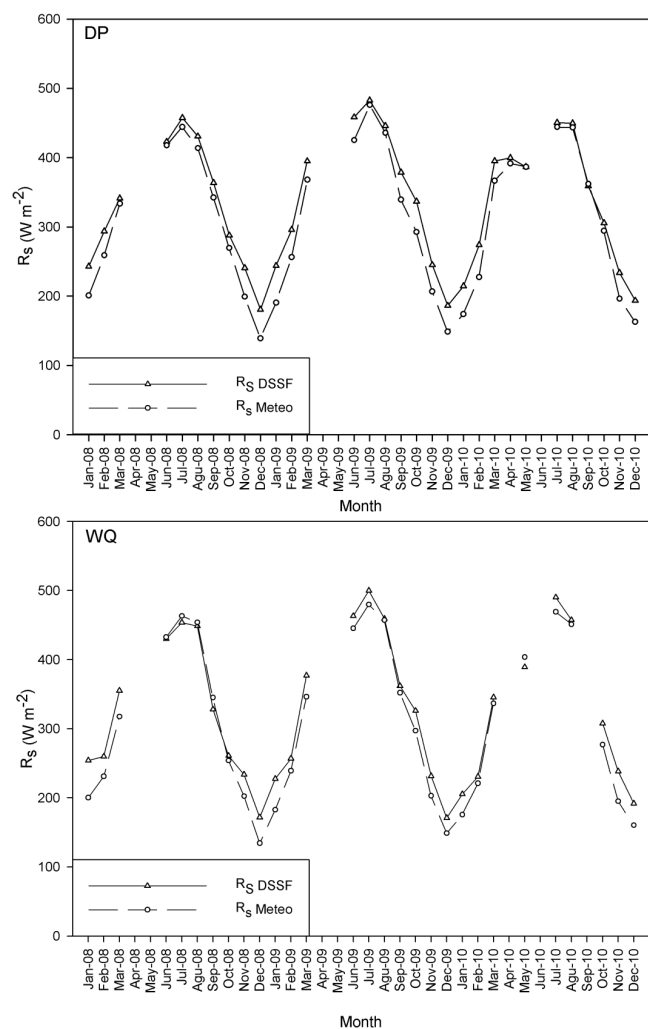


Fig. 6. Examples of monthly DSSF solar radiation (R_s DSSF) and monthly meteorological station solar radiation (R_s DSSF) cycles from 2008 to 2010 at two meteorological stations located in flat conditions (DP) and hilly conditions (WQ).

the most difficult modeling scenario involving hilly terrain under cloudy skies. Satellite-based insolation retrievals can therefore be of significant utility in extrapolating instantaneous clear-sky ET retrievals to daily, monthly and seasonal estimates (Anderson et al., 2012).

7 Conclusions

Hourly, daily and monthly solar radiation estimates derived from the DSSF product produced by LSA SAF using MSG SEVIRI imagery were compared to pyranometer data in two terrain classes (flat and hilly) and for two atmospheric conditions (clear and cloudy sky), as well as for snow and ice cover. In general terms, hourly results compared favorably with the RMSE value from 20 % to 25 % reported previously for global evaluation studies of satellite-based R_s retrievals.

Evaluation yielded good results in flat areas with an averaged model RMSE of 65 W m^{-2} (19 %), 34 W m^{-2} (9.7 %) and 21 W m^{-2} (5.6 %), and good R^2 of 0.95, 0.96 and 0.99, for hourly, daily and monthly-averaged solar radiation and including clear and cloudy sky conditions and snow or ice covers. Sites in hilly terrain also yielded reasonable R^2 of 0.91, 0.93 and 0.96 for hourly, daily and monthly time steps, and averaged model RMSE of 89 W m^{-2} (27 %), 48 W m^{-2} (14.5 %) and 32 W m^{-2} (9.3 %), respectfully. Comparisons at these sites could be improved by applying terrain-based corrections for topographic shadowing at sub-pixel levels. Hourly solar radiation overestimation in cloudy sky conditions and especially over snow and ice cover, could lead to high errors in energy fluxes monitoring in snow-melting related studies. Finally, according to the literature, the LSA SAF solar radiation product can be used as an operative input to calculate evaporative fluxes.

Acknowledgements. Authors would like to thank Miquel Ninyerola, Xavier Pons and Lluís Pesquer from the Autonomous University of Barcelona and Center for Ecological Research and Forestry Applications for his help in solar radiation data filtering.

This research has been developed thanks to a grant funded by the Generalitat de Catalunya, Talència (2009BE200188) and GRUMETS (2009SGR1511) and financial support from the United States Department of Agriculture.

We would like to express our thanks to the SMC (Catalan Meteorological Service) and Department of Territory and Sustainability of the Catalan Ministry that has freely provided us with the solar radiation data from the meteorological stations.

The US Department of Agriculture (USDA) prohibits discrimination in all its programs and activities on the basis of race, color, national origin, age, disability, and where applicable, sex, marital status, familial status, parental status, religion, sexual orientation, genetic information, political beliefs, reprisal, or because all or part of an individual's income is derived from any public assistance program. (Not all prohibited bases apply to all programs.) Persons with disabilities who require alternative means for communication of program information (Braille, large print, audiotape, etc.) should contact USDA's TARGET Center at (202) 720-2600 (voice and TDD). To file a complaint of discrimination, write to USDA, Director, Office of Civil Rights, 1400 Independence Avenue, S.W., Washington, D.C. 20250-9410, or call (800) 795-3272 (voice) or (202) 720-6382 (TDD). USDA is an equal opportunity provider and employer.

Edited by: A. Loew

References

- Allen, R. G., Pereira, L. S., Raes, D., and Smith, M.: Crop evapotranspiration – Guidelines for computing crop water requirements, FAO Irrigation and Drainage Paper, Food and Agriculture Organization of the United Nations, Rome, 1998.
- Allen, R. G., Tasumi, M., and Trezza, R.: Satellite-based energy balance for mapping evapotranspiration with internalized calibration (METRIC) – Model, *J. Irrig. Drain. E-Asce*, 133, 380–394, doi:10.1061/(ASCE)0733-9437(2007)133:4(380), 2007.
- Anderson, M. C., Norman, J. M., Mecikalski, J. R., Torn, R. D., Kustas, W. P., and Basara, J. B.: A multiscale remote sensing model for disaggregating regional fluxes to micrometeorological scales, *J. Hydrometeorol.*, 5, 343–363, 2004.
- Anderson, M. C., Kustas, W. P., Alfieri, J. G., Gao, F., Hain, C., Prueger, J. H., Evett, S., Colaizzi, P., Howell, T., and Chávez, J. L.: Mapping daily evapotranspiration at Landsat spatial scales during the BEAREX'08 field campaign, *Adv. Water Resour.*, 50, 162–177, doi:10.1016/j.advwatres.2012.06.005, 2012.
- Bastiaanssen, W. G. M., Menenti, M., Feddes, R. A., and Holtslag, A. A. M.: A remote sensing surface energy balance algorithm for land (SEBAL) – 1. Formulation, *J. Hydrol.*, 213, 198–212, 1998.
- Bois, B., Pieri, P., Van Leeuwen, C., Wald, L., Huard, F., Gaudillere, J. P., and Saur, E.: Using remotely sensed solar radiation data for reference evapotranspiration estimation at a daily time step, *Agr. Forest Meteorol.*, 148, 619–630, doi:10.1016/j.agrformet.2007.11.005, 2008.
- Brisson, A., Le Borgne, P., and Marsouin, A.: Development of Algorithms for Surface Solar Irradiance retrieval at O&SI SAF low and Mid Latitude, available at: <http://www.eumetsat.int/groups/pops/documents/document/002163.pdf>, 1999.
- Clerbaux, N., Bertrand, C., Caprion, D., Depaepe, B., Dewitte, S., Gonzalez, L., and Ipe, A.: Narrowband-to-Broadband Conversions for SEVIRI, Proceedings of the 2005 EUMETSAT Meteorological Satellite Conference, Dubrovnik, 351–357, 2005.
- Cristóbal, J., Ninyerola, M., and Pons, X.: Modeling air temperature through a combination of remote sensing and GIS data, *J. Geophys. Res.*, 113, D13106, doi:10.1029/2007jd009318, 2008.
- Cristóbal, J., Poyatos, R., Ninyerola, M., Llorens, P., and Pons, X.: Combining remote sensing and GIS climate modelling to estimate daily forest evapotranspiration in a Mediterranean mountain area, *Hydrol Earth Syst Sc.*, 15, 1563–1575, doi:10.5194/hess-15-1563-2011, 2011.
- Diak, G. R., Anderson, M. D., Bland, W. L., Norman, J. M., Mecikalski, J. M., and Aune, R. M.: Agricultural management decision aids driven by real-time satellite data, *B. Am. Meteorol. Soc.*, 79, 1345–1355, 1998.
- Diak, G. R., Mecikalski, J. R., Anderson, M. C., Norman, J. M., Kustas, W. P., Torn, R. D., and DeWolf, R. L.: Estimating Land Surface Energy Budgets From Space: Review and Current Efforts at the University of Wisconsin – Madison and USDA – ARS, *B. Am. Meteorol. Soc.*, 85, 65–78, doi:10.1175/bams-85-1-65, 2004.
- Dickinson, R. E.: Modeling evapotranspiration for three-dimensional global climate models, in: *Climate Processes and Climate Sensitivity*, edited by: Hansen, J. E. and Takehashi, T., American Geophysical Union, Washington, 58–72, 1984.
- Dürr, B., Zelenka, A., Mueller, R., and Philipona, R.: Verification of CM-SAF and MeteoSwiss satellite based retrievals of surface shortwave irradiance over the Alpine region, *Int. J. Remote Sens.*, 31, 4179–4198, doi:10.1080/01431160903199163, 2010.
- Frouin, R., Lingner, D. W., Gautier, C., Baker, K. S., and Smith, R. C.: A Simple Analytical Formula to Compute Clear Sky Total and Photosynthetically Available Solar Irradiance at the Ocean Surface, *J. Geophys. Res.-Oceans*, 94, 9731–9742, 1989.
- Garatza-Payan, J. and Watts, C. J.: The use of remote sensing for estimating ET of irrigated wheat and cotton in Northwest Mexico, *Irrig. Drainag. Syst.*, 19, 301–320, 2005.
- Garatza-Payan, J., Pinker, R. T., Shuttleworth, W. J., and Watts, C. J.: Solar radiation and evapotranspiration in northern Mexico estimated from remotely sensed measurements of cloudiness, *Hydrolog. Sci. J.*, 46, 465–478, doi:10.1080/02626660109492839, 2001.
- Gautier, C., Diak, G., and Masse, S.: A Simple Physical Model to Estimate Incident Solar-Radiation at the Surface from Goes Satellite Data, *J. Appl. Meteorol.*, 19, 1005–1012, 1980.
- Geiger, B., Meurey, C., Lajas, D., Franchistéguy, L., Carrer, D., and Roujean, J.-L.: Near real-time provision of downwelling shortwave radiation estimates derived from satellite observations, *Meteorol. Appl.*, 15, 411–420, doi:10.1002/met.84, 2008a.
- Geiger, B., Carrer, D., Franchistéguy, L., Roujean, J. L., and Meurey, C.: Land Surface Albedo Derived on a Daily Basis From Meteosat Second Generation Observations, *IEEE T. Geosci. Remote*, 46, 3841–3856, doi:10.1109/Tgrs.2008.2001798, 2008b.
- Ineichen, P., Barroso, C. S., Geiger, B., Hollmann, R., Marsouin, A., and Mueller, R.: Satellite Application Facilities irradiance products: hourly time step comparison and validation over Europe, *Int. J. Remote Sens.*, 30, 5549–5571, doi:10.1080/01431160802680560, 2009.
- Jackson, R. D., Reginato, R. G., and Idso, S. B.: Wheat canopy temperature a practical tool for evaluating water requirements, *Water Resour. Res.*, 13, 651–656, 1977.
- Jacobs, J. M., Myers, D. A., Anderson, M. C., and Diak, G. R.: GOES surface insolation to estimate wetlands evapotranspiration, *J. Hydrol.*, 266, 53–65, doi:10.1016/s0022-1694(02)00117-8, 2002.
- Jacobs, J. M., Anderson, M. C., Friess, L. C., and Diak, G. R.: Solar radiation, longwave radiation and emergent wetland evapotranspiration estimates from satellite data in Florida, USA, *Hydrolog. Sci. J.*, 49, 461–476, doi:10.1623/hysj.49.3.461.54352, 2004.
- Janjai, S., Pankaew, P., Laksanaboonsong, J., and Kitichantaropas, R.: Estimation of solar radiation over Cambodia from long-term satellite data, *Renewable Energy*, 36, 1214–1220, doi:10.1016/j.renene.2010.09.023, 2011.
- Journee, M. and Bertrand, C.: Improving the spatio-temporal distribution of surface solar radiation data by merging ground and satellite measurements, *Remote Sens. Environ.*, 114, 2692–2704, doi:10.1016/j.rse.2010.06.010, 2010.
- Kalma, J. D., McVicar, T. R., and McCabe, M. F.: Estimating Land Surface Evaporation: A Review of Methods Using Remotely Sensed Surface Temperature Data, *Surv. Geophys.*, 29, 421–469, doi:10.1007/s10712-008-9037-z, 2008.
- Kustas, W. P. and Norman, J. M.: A two-source energy balance approach using directional radiometric temperature observations for sparse canopy covered surfaces, *Agron. J.*, 92, 847–854, 2000.
- Kustas, W. P., Pinker, R. T., Schmutge, T. J., and Humes, K. S.: Daytime net-radiation estimated for a semiarid rangeland basin

- from remotely-sensed data, *Agr. Forest Meteorol.*, 71, 337–357, doi:10.1016/0168-1923(94)90019-1, 1994.
- LSA SAF: The EUMETSAT Satellite Application Facility on Land Surface Analysis (LSA SAF), Product User Manual, Downwelling Shortwave Flux (DSSF), available at: <https://landsaf.meteo.pt/algorithms.jsp?seltab=1\&starttab=1>, 2010.
- Manabe, S.: Climate and the ocean circulation. I the atmospheric circulation and the hydrology of the earth's surface, *Mon. Weather Rev.*, 97, 739–774, 1969.
- Manalo-Smith, N., Smith, G. L., Tiwari, S. N., and Staylor, W. F.: Analytic forms of bi-directional reflectance functions for application to Earth radiation budget studies, *J. Geophys. Res.*, 103, 19733–19751, 1998.
- Martínez-Durbán, M., Zarzalejo, L. F., Bosch, J. L., Rosiek, S., Polo, J., and Batlles, F. J.: Estimation of global daily irradiation in complex topography zones using digital elevation models and meteosat images: Comparison of the results, *Energ. Convers. Manage.*, 50, 2233–2238, doi:10.1016/j.enconman.2009.05.009, 2009.
- Monteith, J. L.: Evaporation and environment, in: *Proceedings of the 19th Soc. Exp. Biol. Symp.*, 205–234, New York, 1965.
- Ninyerola, M., Pons, X., and Roure, J. M.: A methodological approach of climatological modelling of air temperature and precipitation through GIS techniques, *Int. J. Climatol.*, 20, 1823–1841, 2000.
- Oliphant, A. J., Spronken-Smith, R. A., Sturman, A. P., and Owens, I. F.: Spatial variability of surface radiation fluxes in mountainous terrain, *J. Appl. Meteorol.*, 42, 113–128, 2003.
- Olseth, J. A. and Skartveit, A.: Solar irradiance, sunshine duration and daylight illuminance derived from METEOSAT data for some European sites, *Theor. Appl. Climatol.*, 69, 239–252, doi:10.1007/s007040170029, 2001.
- Orús, J. J., Català, M. A., and Núñez, J.: *Astronomía esférica y mecánica celeste*, Publicacions y Edicions de la Universitat de Barcelona, Barcelona, 2007.
- Otkin, J. A., Anderson, M. C., Mecikalski, J. R., and Diak, G. R.: Validation of GOES-based insolation estimates using data from the US Climate Reference Network, *J. Hydrometeorol.*, 6, 460–475, doi:10.1175/jhm440.1, 2005.
- Paech, S. J., Mecikalski, J. R., Sumner, D. M., Pathak, C. S., Wu, Q. L., Islam, S., and Sangoyomi, T.: A Calibrated, High-Resolution GOES Satellite Solar Insolation Product for a Climatology of Florida Evapotranspiration, *J. Am. Water Resour. As.*, 45, 1328–1342, doi:10.1111/j.1752-1688.2009.00366.x, 2009.
- Pereira, E. B., Abreu, S. L., Stuhlmann, R., Rieland, M., and Colle, S.: Survey of the incident solar radiation in Brazil by use of Meteosat satellite data, *Sol. Energy*, 57, 125–132, doi:10.1016/s0038-092x(96)00059-x, 1996.
- Pinker, R. T. and Laszlo, I.: Effects of Spatial Sampling of Satellite Data on Derived Surface Solar Irradiance, *J. Atmos. Ocean Tech.*, 8, 96–107, 1991.
- Pinker, R. T., Tarpley, J. D., Laszlo, I., Mitchell, K. E., Houser, P. R., Wood, E. F., Schaake, J. C., Robock, A., Lohmann, D., Cosgrove, B. A., Sheffield, J., Duan, Q. Y., Luo, L. F., and Higgins, R. W.: Surface radiation budgets in support of the GEWEX Continental-Scale International Project (GCIP) and the GEWEX Americas Prediction Project (GAPP), including the North American Land Data Assimilation System (NLDAS) Project, *J. Geophys. Res.-Atmos.*, 108, 8844, doi:10.1029/2002jd003301, 2003.
- Pinker, R. T., Zhang, B., and Dutton, E. G.: Do satellites detect trends in surface solar radiation?, *Science*, 308, 850–854, doi:10.1126/science.1103159, 2005.
- Pons, X. and Ninyerola, M.: Mapping a topographic global solar radiation model implemented in a GIS and refined with ground data, *Int. J. Climatol.*, 28, 1821–1834, doi:10.1002/Joc.1676, 2008.
- Pons, X., Cristóbal, J., González, O., Riverola, A., Serra, P., Cea, C., Domingo, C., Díaz, P., Monterde, M., and Velasco, E.: Ten Years of Local Water Resource Management: Integrating Satellite Remote Sensing and Geographical Information Systems, *Eur. J. Remote Sens.*, 45, 317–332, doi:10.5721/EuJRS20124528, 2012.
- Priestley, C. H. B. and Taylor, R. J.: On the assessment of surface heat flux and evaporation using large-scale parameters, *Mon. Weather Rev.*, 100, 81–92, 1972.
- Rigollier, C., Lefèvre, M., and Wald, L.: The method Heliosat-2 for deriving shortwave solar radiation from satellite images, *Sol. Energy*, 77, 159–169, doi:10.1016/j.solener.2004.04.017, 2004.
- Roerink, G. J., Su, Z., and Menenti, M.: S-SEBI: A simple remote sensing algorithm to estimate the surface energy balance, *Phys. Chem. Earth Pt. B*, 25, 147–157, 2000.
- Seguin, B. I. and Itier, B.: Using midday surface temperature to estimate daily evapotranspiration from satellite IR data, *Int. J. Remote Sens.*, 4, 371–383, 1983.
- Stewart, J. B., Watts, C. J., Rodríguez, J. C., De Bruin, H. A. R., van den Berg, A. R., and Garatuza-Payan, J.: Use of satellite data to estimate radiation and evaporation for northwest Mexico, *Agr. Water Manage.*, 38, 181–193, doi:10.1016/s0378-3774(98)00068-7, 1999.
- Su, H. B., McCabe, M. F., Wood, E. F., Su, Z., and Prueger, J. H.: Modeling evapotranspiration during SMACEX: Comparing two approaches for local- and regional-scale prediction, *J. Hydrometeorol.*, 6, 910–922, 2005.
- Zelenka, A., Perez, R., Seals, R., and Renne, D.: Effective accuracy of satellite-derived hourly irradiances, *Theor. Appl. Climatol.*, 62, 199–207, doi:10.1007/s007040050084, 1999.